SAND87-2290

A Final Report on the Phase I Testing of a Molten-Salt Cavity Receiver

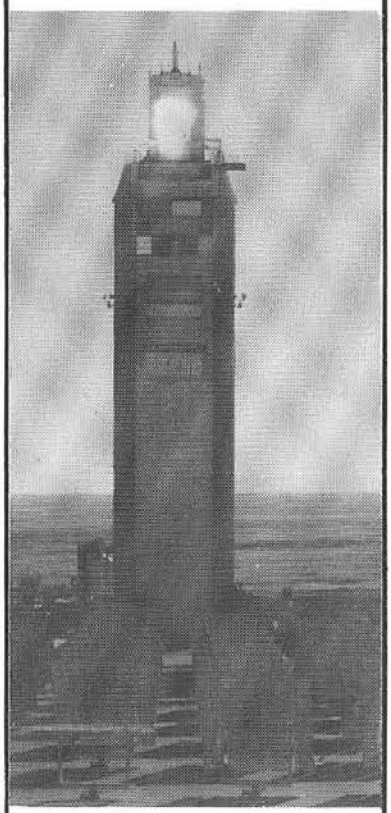

Volume I — A Summary Report

David C. Smith
James M. Chavez

Sandia National Laboratories

Issued by Sandia National Laboratories, operated for the United States Department of Energy by Sandia Corporation.

Printed in the United States of America
Available from
National Technical Information Service
U.S. Department of Commerce
5285 Port Royal Road
Springfield, VA 22161

NTIS price codes
Printed copy: A03
Microfiche copy: A01

Distribution
UC-235

SAND87-2290
Unlimited Release
Printed 1988

A FINAL REPORT ON THE PHASE I TESTING OF A MOLTEN-SALT CAVITY RECEIVER

VOLUME I - A SUMMARY REPORT

David C. Smith*
Nuclear Equipment Division
The Babcock & Wilcox Company
Barberton, Ohio

James M. Chavez
Central Receiver Technology Branch
Sandia National Laboratories
Albuquerque, New Mexico

ABSTRACT

This report describes the successful design, construction, and testing of a solar central receiver using molten nitrate salt as a heat exchange fluid. The receiver is a 4.5-MWt salt-in-tube cavity receiver built as part of the Molten Salt Subsystem/Component Test Experiment. Design studies for large commercial plants (30-100 MWe) have shown molten salt to be an excellent fluid for solar thermal plants as it is a good medium for efficient thermal storage. The properties that make molten salt a good medium for storage, however, make receiver design challenging. This test program was recommended by the utility- and industrial participants to address uncertainties in commercial receiver designs. The receiver was designed to incorporate features of commercial receiver designs. The test program was managed by Sandia National Laboratories for the U.S. Department of Energy. The receiver was fabricated off-site and then installed at Sandia National Laboratories' Central Receiver Test Facility in Albuquerque, New Mexico. Solar testing was conducted during a six-month period. The purpose of the testing was to characterize the operational capabilities of the receiver under solar and stand-by conditions. This testing consisted of initial check-out of the systems, followed by steady-state performance, transient receiver operation, receiver operation in clouds, receiver thermal loss testing, receiver start-up operation, and overnight thermal conditioning tests. This report describes the design, fabrication, ar results of testing of the receiver.

*Currently with Science Applications International Corp., Albuquerque, NM

ACKNOWLEDGMENT

We would like to acknowledge and express our appreciation to all those who contributed to the program. They include authors of Volume II:Appendix 1-The Main Report: Patricia Bator and Phil Reed of the Babcock & Wilcox Company, Stan Saloff, Mark (Buzz) Lanning, and Gene Riley of the McDonnell Douglas Company, Bob Boehm of the University of Utah, Russ Skocypec of Sandia National Labs, and Gio Carli of Foster Wheeler. In addition, we would like to acknowledge the following personnel whose contributions made the program successful.

SANDIA NATIONAL LABORATORIES

Nina Bergan	Marty Hall	Hal Norris
Ken Bolt	John Holmes	John Otts
Bob Bradshaw	Jay Holten	Anne Poore
Nova Carter	Jim Grossman	Vince Romero
Bill Couch	Jim Imboden	Al Skinrood
Bill Delameter	Sam Jenkins	Milt Stomp
Sam Dunkin	Roy Johnston	Jack Swearengen
Bob Edgar	J.J. Kelton	Kathy Tate
Boe Ellis	Rod Mahoney	Arleen Vance
Lindsey Evans	Matt Matthews	Craig Tyner
Paul Flora	Clay Mavis	Bill Wilson

BABCOCK & WILCOX

Wes Allman	George Grant	Joe Stadelman
Gene Campbell	Vic Leshock	John Swank
Jim Clevenger	Earl Livingston	Candy Woodruff
Arlis Cooper	Earl Martin	Dan Young
Ralph Dowling	Byron Pritchard	Tom Fewell
Karen Sluka	Curt Flora	Mark Smith
Chuck Getz	Charlie Somers	

McDONNELL DOUGLAS

Bob Gervais	Chick Finch	Tom McKowen
Dave Carey	Matt Russell	
Gerry Coleman	John Navickus	

FOSTER WHEELER

Rich McMillan	Tom Staed

ARIZONA PUBLIC SERVICE

Dale Thornburg	Eric Weber

SOUTHERN CALIFORNIA EDISON

Paul Skavarna	Charles Trilling	Chuck Lopez

BLACK & VEATCH

John Harder	Larry Durbal

CONTRACTORS

George Mulholand	Tom Tracy

VOLUME I - A SUMMARY REPORT

TABLE OF CONTENTS

VOLUME I - A SUMMARY REPORT

LIST OF FIGURES

LIST OF TABLES

FOREWORD

This report is of work funded by the U.S. Department of Energy under Contract DE-AC04-76DP00789. The report is published in three volumes:

Volume I	--	A Summary Report
Volume II	--	Appendix 1 - The Main Report
Volume III	--	Appendices A - J

The research and development described in this report was conducted within the U.S. Department of Energy's (DOE) Solar Thermal Technology Program. The goal of the Solar Thermal Technology Program is to advance the engineering and scientific understanding of solar thermal technology, and to establish the technology base from which private industry can develop solar thermal power production options for introduction into the competive market.

In a solar thermal system, mirrors or lenses focus sunlight onto a receiver where a working fluid absorbs the solar energy as heat. The system then converts the energy into electricity or uses it as process heat. There are two kinds of solar thermal systems: central receiver systems and distributed receiver systems. A central receiver system uses a field of heliostats (two-axis tracking mirrors) to focus the sun's radiant energy onto a receiver mounted on a tower. A distributed receiver system uses three types of optical arrangements-parabolic troughs, parabolic dishes, and hemispherical bowls-to focus focus sunlight onto either a line or point receiver.

This report describes the design, construction, testing, and evaluation of a solar central receiver that uses molten nitrate salt as a heat transport fluid. The receiver is a 4.5 MWt salt-in-tube cavity receiver that is a scaled down version of a commercial receiver design. This development and test program was carried out by a team of companies on a cost-shared basis with the DOE. The receiver was tested at Sandia National Laboratories' Central Receiver Test Facility in Albuquerque, New Mexico.

1.0 INTRODUCTION

1.1 Background

A 4.5-MWt salt-in-tube cavity receiver was designed, built, and tested as part of the U.S. Department of Energy (DOE) solar thermal research program. In the last 10 years many studies and test programs have been carried out to develop and demonstrate the viability of molten-salt central receiver power plants [1,2,3,4]. Molten nitrate salt (60% sodium nitrate and 40% potassium nitrate, by weight) is used as the working fluid because its high density and specific heat make it attractive for thermal storage systems, and it is chemically stable at elevated temperatures. A preliminary design study was performed by Arizona Public Service (APS) Company in 1983 for the repowering of a fossil-fuel plant (Saguaro) with a molten-salt central receiver and steam generator [5]. This study recommended a development plan to reduce the technical risk of building a central receiver power plant. The APS study recommended the fabrication and testing of a scaled-down salt-in-tube receiver with features planned for the Saguaro receiver design. Responding to this recommendation, DOE authorized the Molten-Salt Subsystem/Component Test Experiment (MSS/CTE) Program (also called the Repowering Category B Program) with contracting and technical management by Sandia National Laboratories. The MSS/CTE program consists of three experiments:

- A 4.5-MWt Receiver Test
- A Valve Seal Bench Test
- A Pump and Valve Test

This report presents the 4.5-MWt Receiver Test, including the design, fabrication, erection, testing, and test results. Separate reports will be prepared for the other tests. The MSS/CTE program was carried out by a team of companies on a cost-shared basis with the DOE. Babcock & Wilcox acted as prime contractor for the program with the following subcontractors:

- Arizona Public Service Company
- McDonnell Douglas
- Black & Veatch
- Foster Wheeler
- Southern California Edison

The receiver was tested at Sandia's Central Receiver Test Facility (CRTF) in Albuquerque, New Mexico.

1.2 Objectives of the Program

The test program was implemented to address technical concerns about commercial receiver designs by designing, fabricating, and testing a scaled-down receiver.

The first objective of the receiver test program was the design and fabrication of a scaled-down receiver with the major features planned for the Sagurao receiver. The technical objectives of the receiver testing were to (1) confirm the receiver's design by demonstrating its operation and control during conditions expected in commercial solar plants, (2) measure the receiver's

thermal performance, and (3) define the receiver's capabilities during start-up and cloudy conditions. These objectives were met during 20 weeks of testing.

1.3 Description of the Central Receiver Test Facility

The CRTF consists of a field of 221 heliostats (191 were used in the receiver testing) each with 37.2 m^2 (400 ft^2) of mirror surface. A 61-m (200-ft) tower is situated south of the field. More than 5 MWt of solar power can be focused onto a test receiver located on the tower [6]. The facility includes a molten-salt storage and pumping system, with a heat rejection system consisting of a steam generator for cooling the salt, and a condenser and cooling towers for rejecting the heat [7]. The receiver test employed all of these systems.

2.0 DESCRIPTION OF THE RECEIVER

The concept of a commercial molten-salt central receiver system is shown in Figure 1. The sun's energy is reflected by heliostats onto a receiver, which is mounted on a tower. Molten salt is heated in the receiver and sent to the storage system's hot tank. Hot salt is pumped to the steam generator subsystem, where steam is produced for generation of electricity in the turbine generator. The two-tank storage system provides a buffer between the solar receiver and the steam generating subsystem to provide operating flexibility.

FIGURE 1
CONCEPT OF A MOLTEN-SALT CENTRAL RECEIVER SYSTEM

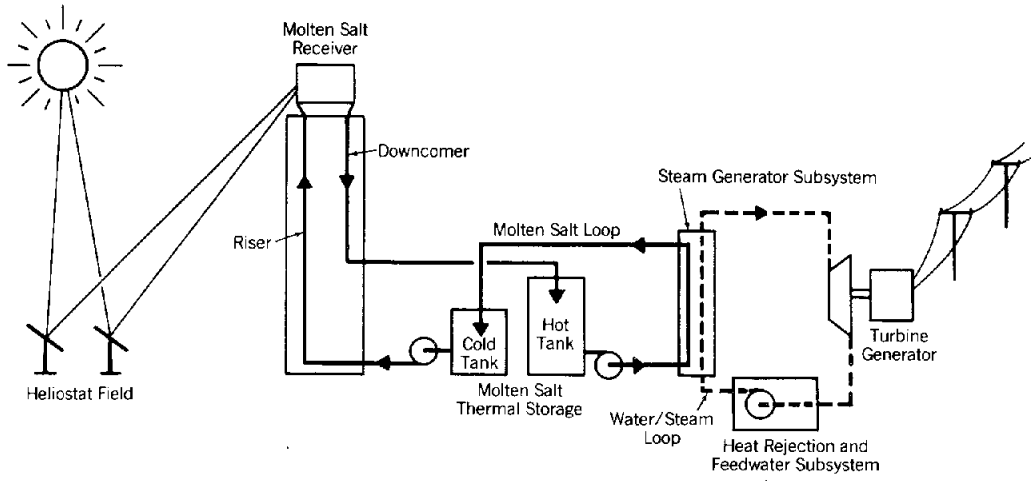

2.1 Design of the Receiver

The receiver illustrated in Figure 2 is designed to employ the key features of the commercial receiver designs [1,2]. These features include:

- a "C" shaped cavity
- "wing" panels in the aperture plane
- tangent tube wall construction
- heat absorption panels hung from the top with lateral supports
- sizing based on flux limits derived from creep/fatigue analysis
- cavity doors to reduce heat loss during stand-by periods
- two flow control zones
- automatic salt outlet temperature control

The receiver is installed atop the CRTF tower and connected to a molten-salt storage subsystem on the ground. Hot salt produced in the receiver is run through a molten-salt steam generator that was installed at the CRTF for a previous experiment [8]. Since this was only a test of the receiver, the energy collected during the test was rejected to the atmosphere.

FIGURE 2
ARTIST'S CONCEPT OF THE RECEIVER

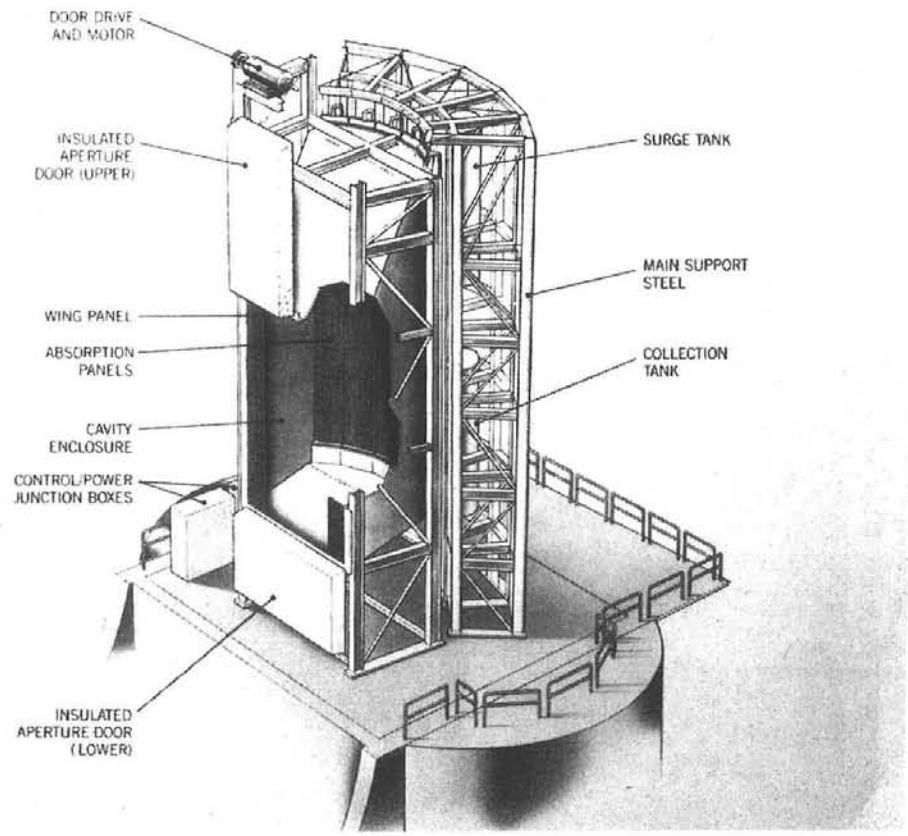

The overall design conditions for the receiver are presented in Table I.

TABLE I

DESIGN CONDITIONS FOR THE RECEIVER

Full Load Absorbed Power	4.5 MWt
Salt Inlet Temperature	288°C (550°F)
Salt Outlet-temperature	566°C (1050°F)
Full Load Salt Flow	43. x 10^3 kg/h (94. x 10^3 lbm/h)

The receiver, shown in Figures 3 and 4 is a north-facing cavity receiver. The cavity aperture faces north toward the CRTF collector field as shown in Figure 3. Under good solar conditions, 5 MW_t of thermal power is focused into the receiver aperture using 191 heliostats from the field. The shape of the cavity is designed to allow the majority of the incoming solar flux to be spread over the larger absorbing surface (to be refered to as the "back panels") while limiting the radiant emission to that leaving the smaller aperture. "Wing" panels are located on each side of the aperture to catch solar flux that does not enter the aperture. The wing panels are used to preheat the salt before it enters the back panels.

FIGURE 3
AERIAL PHOTOGRAPH OF THE CRTF
(with the cavity receiver on the tower)

FIGURE 4
PHOTOGRAPH OF THE RECEIVER
(with heliostats focused on the receiver)

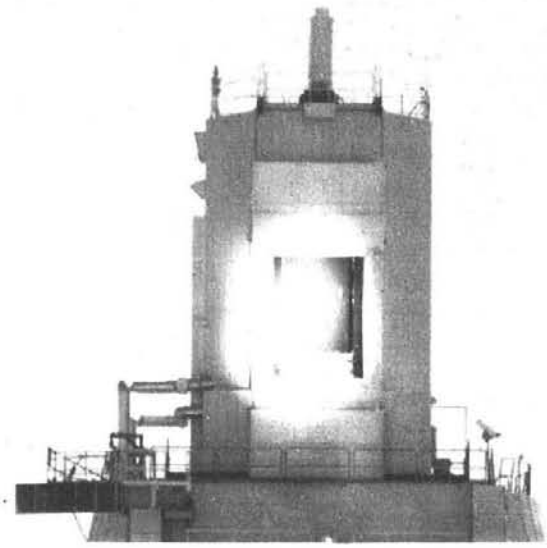

The heat absorption panels on the back wall are composed of 19-mm (3/4-in.)-diameter Alloy-800 tubes. Alloy-800 tubes are used because of the high heat flux and temperatures that are encountered on the back panel. The tubes are painted with a black ceramic paint to increase their absorptivity. The paint used is Pyromark Series 2500 [9] manufactured by Tempil.[1] The tubes are divided symmetrically into two control zones, east and west. Each zone consists of 16 passes of 6 tubes each. The wing panels are made of 25-mm (1-in.) diameter 316-stainless-steel tubes and are also painted with black Pyromark paint. Each wing panel is divided into two passes of 6 tubes each. The passes of both the east and west zones are numbered from 1 to 18 as shown in Figure 5. Salt flow in the receiver follows a serpentine flow path through each of the two control zones as shown in Figure 6.

The multiple-pass arrangement is designed to efficiently transfer heat to the molten salt. Because of the high product of heat capacity and density for the salt, the volume flow rate in the receiver is relatively small (for a given absorbed power). High-velocity flow, however, is important to achieve relatively high heat-transfer coefficients inside the receiver tubes because of the salt's low conductivity. The multiple-pass arrangement channels each zone's total flow through just 6 tubes per pass to create high velocities.

1. Tempil Division, Big Three Industries, Inc., South Plainfield, NJ.

FIGURE 5
LAYOUT OF THE RECEIVER CAVITY

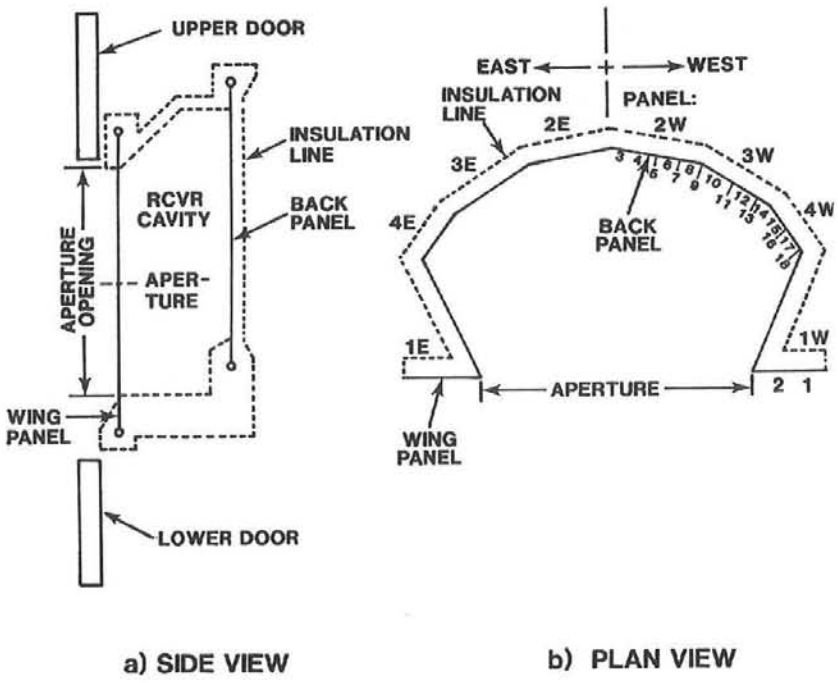

a) SIDE VIEW b) PLAN VIEW

FIGURE 6
SERPENTINE FLOW PATH IN THE RECEIVER

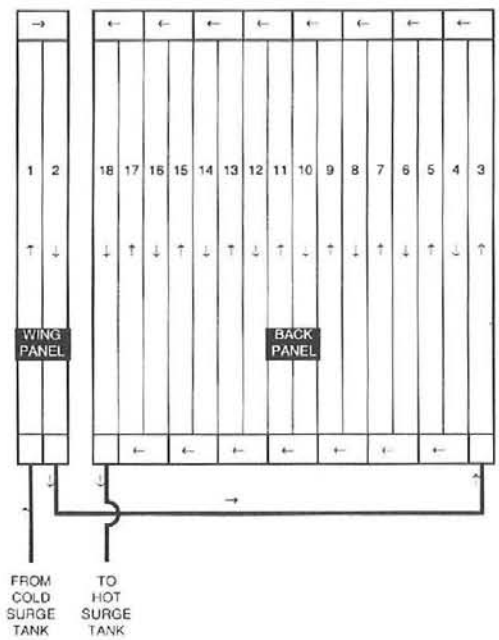

The choice of materials for salt piping was based primarily on their high-temperature strength and resistance to corrosion by the molten-salt. For temperatures below 400°C (750°F), low-carbon steel was employed. Above this temperature, 304 stainless steel was used for corrosion resistance and increased strength. For the back panel tubes, where heat flux is high, Alloy 800 was used for increased resistance to creep and fatigue.

The piping system, tanks, and valves are electrically heated and insulated to prevent freezing of the salt during fill and drain operation, and in stagnant regions, such as instrument lines. Mineral-insulated heat-trace cable is employed for heating and is covered by high-temperature fibrous blanket insulation. Much of the heat-trace design follows recommendations about heat trace by Holmes [10]. All piping is sloped to provide for gravity drainage of the system.

2.2 Sizing the Receiver

The test receiver panels are designed for a life of 30 years, to be typical of a commercial design. The Saguaro commercial receiver was designed for 10,000 daily start-ups, and 40,000 cycles due to cloud passage, which was to represent a 30 year design life. Thermal stress occurs in panels as a result of absorbed heat flux. This stress results in fatigue of the tubes because of the cyclic nature of daily operation and cloud passage. In addition, operation at high temperature causes damage due to the effect of creep. The combined damage from these two effects was calculated by the methods prescribed in ASME Code Case N-47 [11]. This code case provided fatigue limits for Alloy 800 based on isothermal continuous cycling. The test receiver's back panel was designed to match the thermal stresses of the Saguaro commercial receiver. This led to the selection of the 16-pass design, using six tubes in each pass. The tubes were 1.9 mm (3/4 in.) in diameter with a 0.165-mm (.065-in.) wall thickness. The temperature and stress profiles for both the Saguaro receiver and the test receiver are presented in Figure 7, which illustrates the similarity.

Since the original design work was performed, a more quantitative study of cloud cycles based on data from the Solar 1 plant has been performed [12]. This study indicates that the cumulative effect of partial cloud cycles is equivalent to 20,000 full cloud cycles. Also, more recent investigations of Alloy 800 have indicated that thermally induced fatigue is more damaging than isothermal (mechanically induced) fatigue; [13], however, the material test results are preliminary and therefore are not accounted for in this report.

Flux limits for the receiver are derived based on the fatigue limits of the tube material and the maximum allowable salt-metal interface temperature of 593°C (1100°F). The flux limit for the receiver is presented in Figure 8. Both the original design limit and the limit based on the lower number of cycles and revised fatigue properties are presented. The predicted heat flux (from the McDonnell Douglas CONCEN program) is presented as well. The test receiver cavity was sized and configured to achieve heat fluxes that approached but were below the original limit.

FIGURE 7
THERMAL STRESSES ON THE PANEL

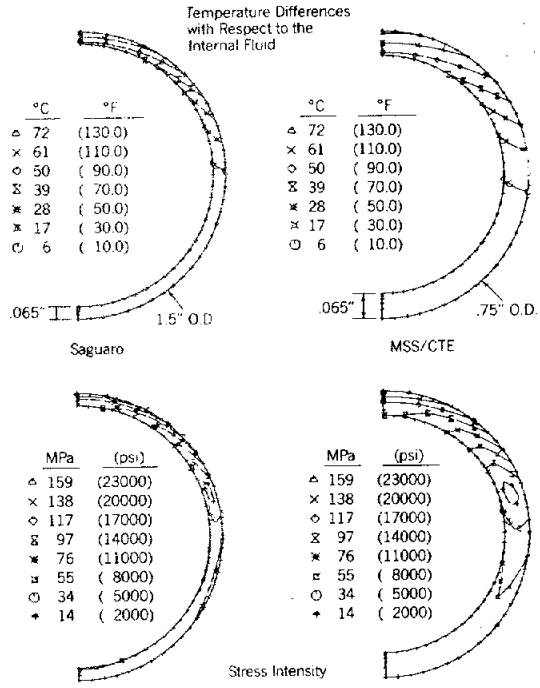

FIGURE 8
FLUX LIMIT OF THE RECEIVER

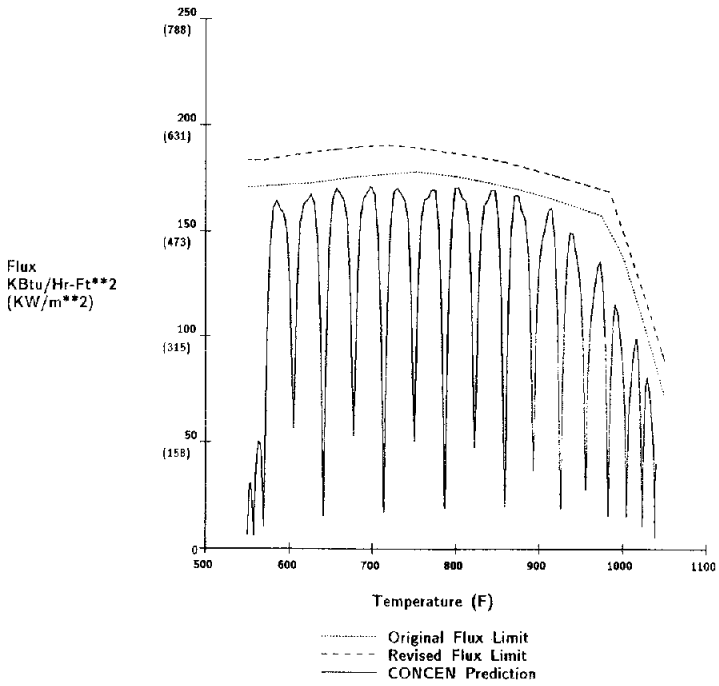

2.3 Design of the Heat Absorption Panel

The receiver employs two different back panel designs, one developed by Babock & Wilcox (Figure 9a) and the other by Foster Wheeler (Figure 9b). Although the thermal/hydraulic aspects of the panels are the same, the mechanical designs differ.

FIGURE 9
RECEIVER PANELS

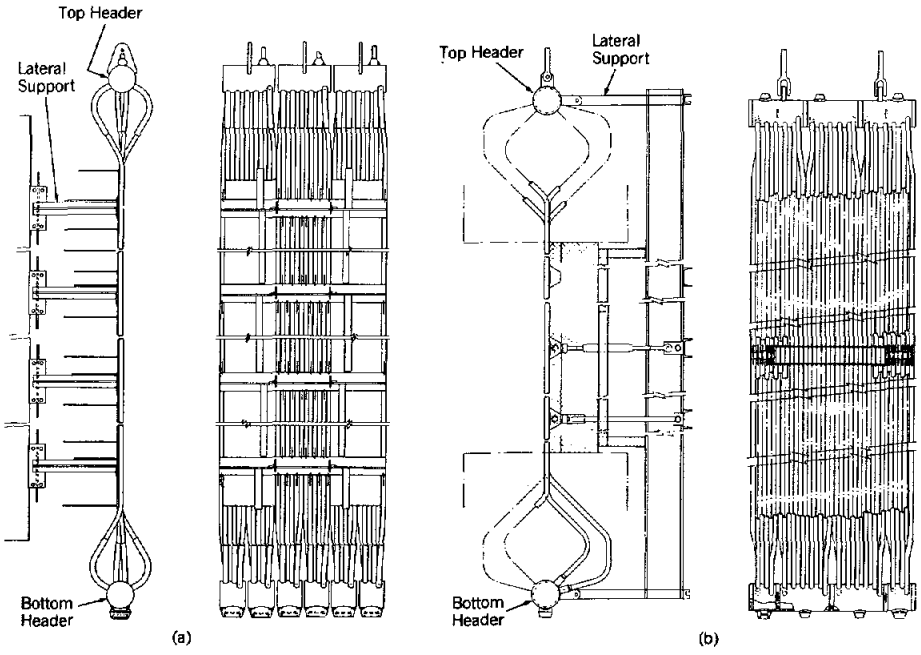

The lateral supports of both designs serve to restrain deflection of the tubes caused by internally generated thermal stresses. The restraints also serve to transmit wind loads, precluding potential vibration of the panels. The dead weight of both types of panels is suspended from lugs in the top header to permit unrestricted thermal expansion.

The back of each panel is insulated with 20.32 cm (8 in.) of ceramic-fiber blanket insulation attached to the lateral supports and wired into place. The front of each panel is painted with high-temperature black paint to increase the panel's absorptivity. The floor, ceiling, and side walls of the cavity are also lined with 20.32 cm of ceramic blanket insulation to limit conduction heat loss from the cavity.

The two panels differ in the design approach to allow for longitudinal growth. The Babcock & Wilcox panel employs a system of rollers (Figure 10a) to allow for longitudinal growth, with divided lower headers to allow for differential expansion of adjacent flow passes. The Foster Wheeler panel (Figure 10b), uses a system of rotating links for longitudinal growth. This panel has a solid lower header with divider plates and large tube bends at the header connections to allow flexibility for pass-to-pass expansion.

FIGURE 10
DESIGN OF THE LATERAL SUPPORT

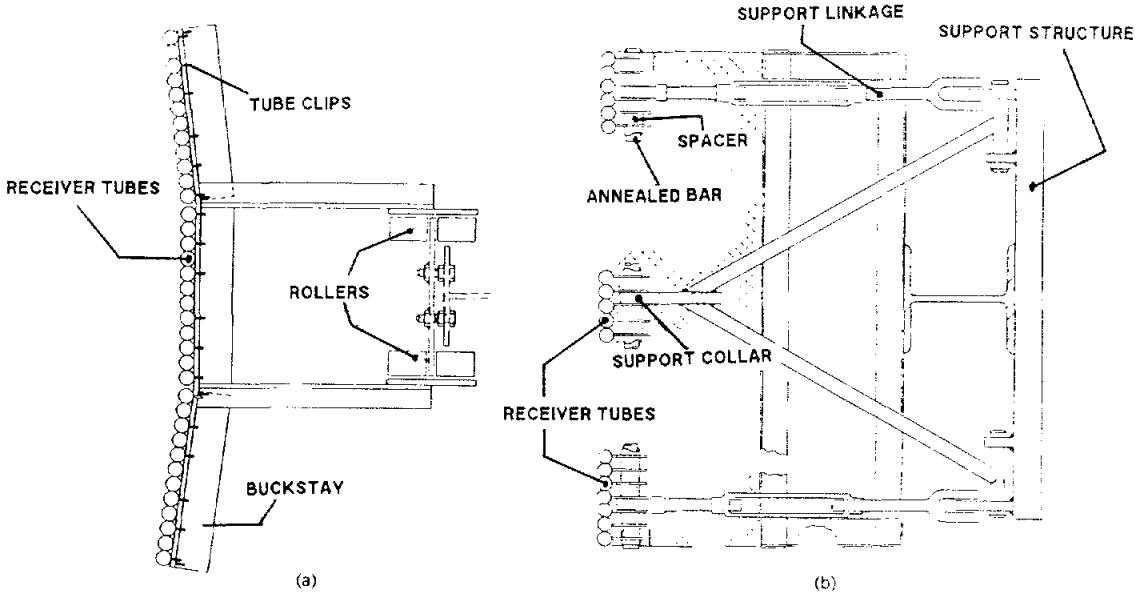

Babcock and Wilcox Foster Wheeler

Tube attachments also differ for each design. The Babcock & Wilcox design uses an alternating (top and bottom) clip arrangement capturing a "T" section horizontal support (Figure 11a). The Foster Wheeler design utilizes tube clips welded to each tube through which a bar passes (Figure 11b).

2.4 Receiver Support Systems

Salt is supplied to the receiver from the existing salt storage and pumping system on the ground. This system feeds the 1.1-m^3 (40-ft^3) cold-salt surge tank in the receiver. Flow from the surge tank is divided to supply flow to the control valves at the inlet of east and west control zones. These valves throttle the flow to control the receiver zone's outlet-salt temperatures. Flow leaving the absorption panels is mixed in the hot-salt surge tank. From here the flow is returned to the storage system on the ground. Figure 12 is a schematic diagram of the receiver that illustrates the flow path and the receiver's instrumentation.

FIGURE 11
TUBE ATTACHMENT

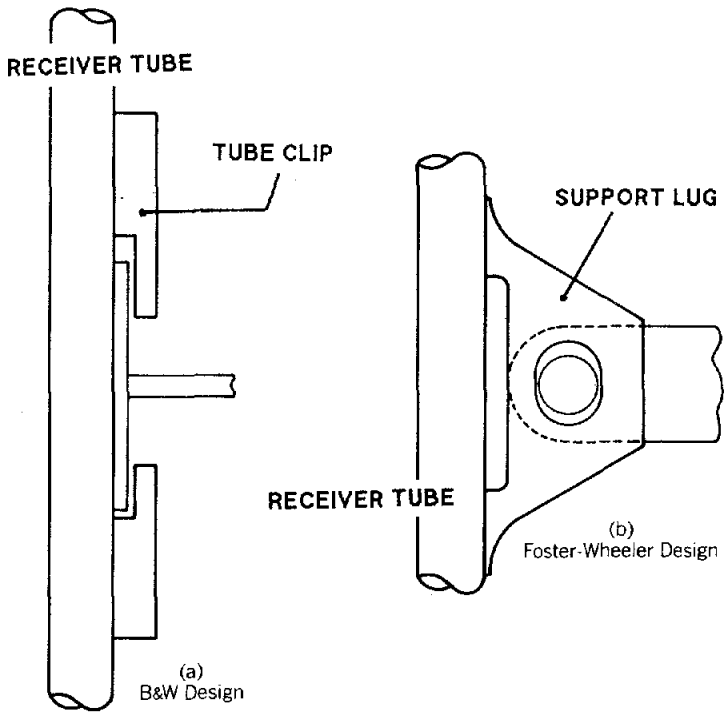

Auxiliary piping in the receiver includes lines to allow filling and draining the receiver, and a circulation line between the cold surge tank and the upper header.

Electrical heat-trace cable is applied to all piping and valves to heat them above the melting point of salt. The salt is fully molten at 243°C (470°F). The heat trace was operated to maintain piping above 273°C (525°F) to allow margin for cold spots. The heat-trace cable was sized to exceed the capacity required to maintain the pipe temperature above the 273°C limit. Active on/off control based on thermocouples attached to the piping was employed to maintain the desired pipe temperatures. The system was divided into approximately 60 zones, each independently controlled in this manner. The heat trace allows flow to be started in the receiver without freezing salt in the lines; however, this heat trace represents a significant parasitic loss for the receiver.

The receiver's instrumentation, shown in Figure 12, includes flux gauges, thermocouples, level transmitters, strain gauges, pressure transmitters and flow meters. They feed back into a distributed digital control system both to facilitate control and to be recorded for later analysis.

FIGURE 12
SCHEMATIC OF THE RECEIVER SUBSYSTEM

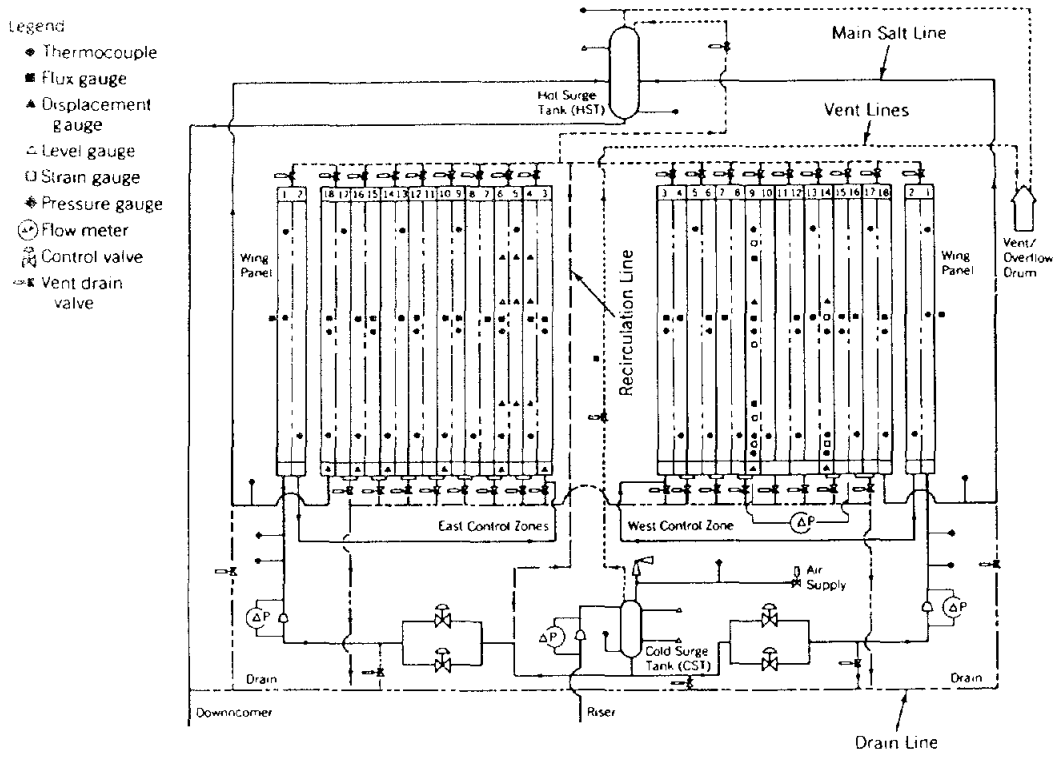

A two-piece insulated door is provided at the cavity aperture to seal the cavity and minimize heat loss during periods when salt flow is maintained but when solar energy is not available, e.g., overnight and when clouds pass. During these periods, the door may be closed and salt flow maintained, eliminating the need to drain the receiver and restart salt flow when the sun returns. In order to maintain overnight salt flow, routing salt from the cold surge tank to the upper panel vent line allows downflow of salt in each panel. Salt flow from each panel is collected in a lower drain header and returned to the downcomer. This flow path minimizes the pumping requirement for salt circulation and eliminates regions where cold salt could stratify.

2.5 Controls and Instrumentation

Four automatic control loops are provided: cold surge tank level, hot surge tank level, and outlet temperature control for each of the two control zones. Level control in the surge tanks is accomplished by simple feedback control of a valve in the riser line (for cold surge tank level) and in the downcomer line (for hot surge tank control). Flow control in the receiver is accomplished using a much more sophisticated control algorithm. Precise control of the receiver's outlet temperature is required to limit exposure of the receiver tubes to corrosive high-temperature salt, while maximizing the true usefulness of the salt by keeping the outlet temperature high.

The control algorithm, shown as a block diagram in Figure 13, uses heat-flux sensors mounted in receiver panels between tubes to measure the flux incident on the panels. In addition, thermocouples attached to the back of the tubes monitor the salt's temperature as it passes through the receiver. Both flux signals and back-tube temperature signals feed into the algorithm as anticipatory signals. The outlet temperature is also measured and used as a feedback signal. In order to obtain the optimal response from the control algorithm, the inputs to the controller (i.e., gains and time constants) were adjusted. This adjustment of the inputs to the controller is referred to later in the text as "tuning."

Two types of flux gauges are employed to measure incident flux on the receiver panels. The primary set of gauges employs a passive cooling system, with a large copper body extending through the receiver's insulation and a finned heat sink to keep the gauge cool. A back-up set of flux gauges has bodies cooled by water.

Salt flow in each of the control zones and total flow are measured using venturi flow meters and pressure transmitters. Redundant level sensors are used in each of the surge tanks, and instrumentation is provided to measure panel displacements, panel strain, and inlet pressure to each control zone. Instrument locations are shown in Figure 12.

3.0 FABRICATION OF THE RECEIVER

3.1 Shop Fabrication

The bulk of the receiver was shop fabricated as a "module," which included the receiver's cavity panels, wing panels, panel supports, and the structural steel frame required to support it. The module was sized for shipment by truck as a unit to the CRTF. The hot and cold surge tanks and their additional support structure were also shop fabricated and shipped to the test site for erection.

3.2 Erection of the Receiver

At the CRTF test site, the tower consists of a 61-m (200-ft) tall, reinforced concrete shell, housing a large "lifting module." This module is placed at ground level for assembly of test receivers, then lifted to the top of the tower for testing. Upon arrival at the CRTF, the receiver module, supporting structure, tanks, and interconnecting piping were assembled on the lifting module. Figure 14 shows assembly of the receiver at ground level. Electrical

FIGURE 13
RECEIVER TEMPERATURE CONTROL ALGORITHM

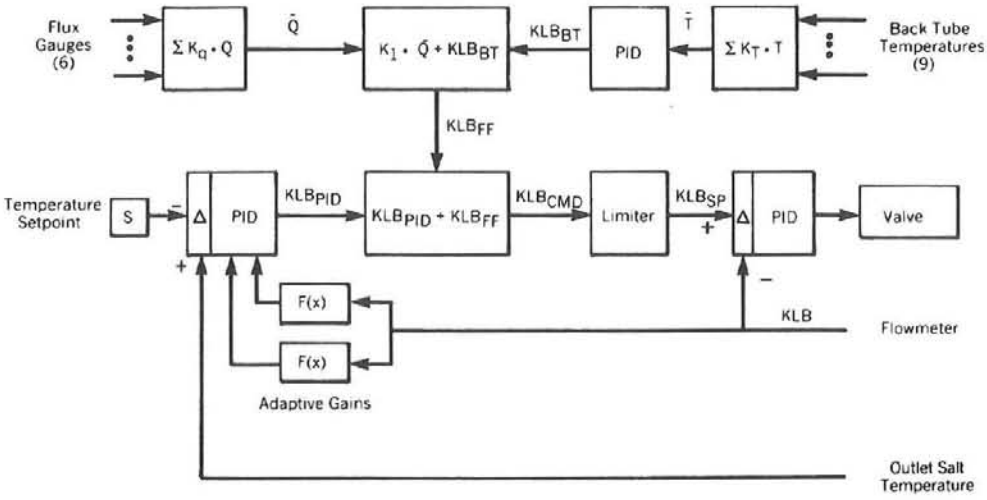

FIGURE 14
RECEIVER ASSEMBLY AT BASE OF TOWER

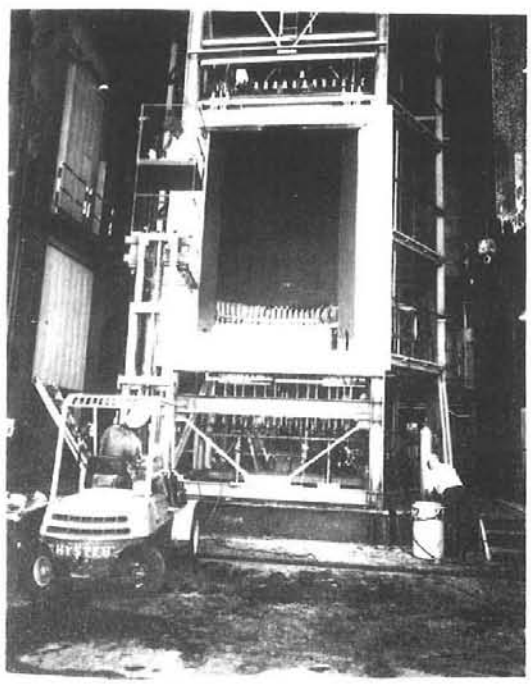

heat trace and insulation were then installed, along with receiver's instrumentation. The instrumentation and the active components of the receiver, such as the doors and valves, were checked out at ground level. The receiver was then lifted to the top of the tower, where final connections and checkouts were performed.

4.0 DESCRIPTION OF THE TEST PROGRAM

4.1 Objectives of the Test Program

The objectives of the receiver test program can be broken down into three categories:

- Confirmation of the Design
- Measurement of Thermal Performance
- Definition of Capabilities

Confirmation of the Design: Confirmation of the design is important to verify that the methods used are valid and could be applied to a scaled-up receiver. Specific aspects include confirmation that the cavity is sized and configured properly so that heat flux is within the established limits, that the thermal expansion system works, allowing the panels to grow, and that the controls and instrumentation function as they should. Any problems with the methods used to fabricate the receiver or in support systems, such as heat trace or valves, can also be expected to reveal themselves during testing.

Measurement of Thermal Performance: The receiver's thermal efficiency was measured for comparison with the design predictions. This allows the methods to be verified and increases the confidence that commercial receivers will perform as expected.

Definition of Capabilities: The test program was also designed to define the capabilities of the receiver when operating under off-design conditions. Tests were conducted to define how well the receiver operates in cloudy conditions, to compare methods of temperature conditioning of the receiver overnight, and to investigate methods to start the receiver in the morning.

These areas are important to designers of subsequent scaled-up receivers, as they confirm the current design methods, or indicate areas where improvements are required. They also give an indication of the expected performance and capabilities of a scaled-up receiver.

4.2 Description of the Test

The initial phase of testing was done to check the operation of the receiver's systems and to perform preliminary "tuning" of the salt flow and temperature controls. During this phase, problems with the salt pumps and instrumentation were corrected, the receiver's absorption surface was painted, and the paint was cured.

Following the check-out phase, the operational test phase was started. During this phase, six types of tests were conducted:

1. Test of Steady-State Performance
2. Test Simulating Cloud Transients
3. Test of Thermal Loss -- Flux-Off and Flux-On
4. Operation During Natural Cloud Transients
5. Development of an Optimum Receiver Start-Up
6. Test of Overnight Thermal Conditioning

A brief description of each test follows.

Test of Steady-State Performance: The receiver was operated with full collector field power from early morning to late afternoon. Data from several days of operation were taken to allow the data to be normalized and averaged so that a "typical" day's performance could be derived. Data from this test were used to confirm that the design was working properly, and to evaluate thermal performance.

Test Simulating Cloud Transients: To perform final control tuning of the receiver's control-algorithm, partial-power cloud transients were simulated. This was done by moving half of the heliostats in the field to 'standby', then returning them to the receiver. These data were used to evaluate the performance of the receiver controls for mild transients. Following this, testing was performed with a simulated east-to-west cloud. To do this, the heliostats were sequenced off the receiver one column at a time, moving from east to west, simulating a sharp-edged cloud moving east to west at 2.4 m/s (8 ft/s). Once they were all off, they were commanded back on in the same fashion. This provided a worst case transient and allowed the testing of several modifications to the controls, with a common input. This test was used to define the capabilities of the controls and to observe the response of the receiver.

Test of Thermal Losses -- Flux-Off and Flux-On: To characterize the performance of the test receiver, thermal losses were measured with the receiver door closed, with the door open but with no flux on the receiver (both flux-off tests), and with the receiver operating near the design point (flux-on). The flux-off tests provided data for losses occurring when the receiver was in a standby mode, and the flux-on test provided data for determining operating losses. For flux-off testing, losses were inferred from the salt's flow rate and temperature drop. For the flux-on case, the receiver was operated at full collector field power and at 50% power with two complementary groups of heliostats. Receiver losses were then inferred from the difference in absorbed power between full-field operation and operation with the two groups. This method is also called the "method of complementary collector partitions" [14]. Results of this test characterize the thermal performance of the receiver.

Operation During Natural Cloud Transients: The capability of the receiver's outlet-temperature controls to perform was evaluated under real conditions during operation in natural clouds. These tests confirmed that the receiver's control algorithm and equipment could perform their intended function.

Development of Optimum Receiver Start-Up: Two methods are available to start this receiver at sunrise. The first involves focusing a select group of heliostats on the receiver panel to warm it above the freezing temperature of salt. Then the receiver is filled, the flow initiated, and the full-field brought on-target. The alternative is to heat the cavity with the door closed and establish salt flow before sunrise. Then the door can be opened and the full-field brought on-target at sunrise. Both start-up methods were tested and the results allow definition of the energy collected and consumed by the two methods.

Overnight Conditioning: As discussed above, one method of starting the receiver is to heat the cavity with the door closed, which allows flow to be started before sunrise. Two methods were tested for overnight heating of or 'conditioning' the cavity. The first employed electric heaters mounted in the cavity floor, which were operated to maintain the cavity's temperature. The second method employed circulating salt through the receiver from the storage system on the ground. This method substituted stored solar thermal energy for electric cavity heat. In addition, the circulating salt eliminated the need to operate most of the electric heat trace on the receiver piping as well as that on the piping in the tower. This significantly reduced electrical parasitics.

Circulation of the molten salt from the ground was accomplished using the main salt pumps. Because of this, an operating crew was required to monitor the system, and testing was performed during daylight hours.

5.0 EVALUATION OF TEST RESULTS

The results of the test were evaluated in line with the objectives of the test program. Discussion of the results relevant to each of the primary objectives is presented below.

5.1 Confirmation of the Design

The design methods employed for the receiver are the same as would be used to design a commercial-scale receiver. Results of the test are evaluated below to confirm that these methods are valid.

Flux Limits of the Panel: To insure that a receiver lasts the required lifetime, the design limits must not be exceeded. For this receiver, the mechanical service design limits are based on the material fatigue limits of the receiver panel. The receiver's panels develop thermal stresses as a result of being heated by the sun and cooled by the salt. During the receiver's design, flux limits were set for the receiver's panel based on daily cycling between operation and shutdown, and the cavity was sized and configured based on these limits. The flux limit varies within the

receiver panel as a function of the salt's temperature. Figure 15 presents the flux limits set in the design, the heat flux predicted for the design, and the values measured in the steady-state tests at solar noon. Test values have been normalized to full-power (4.5-MWth) operation. It appears from the data that the receiver fluxes are generally in agreement with the peak design flux predictions. However, some measured values exceed the predictions, and a few values exceed the allowable flux limit. Based on differences between calibrations of the flux gauges made before and after service in the receiver, the accuracy of the gauges was found to be approximately ± 15%. Therefore, some possibility exists that the limits are being exceeded. Designers of future receivers should bear in mind that tools for predicting receiver flux, while generally correct, cannot be confirmed with a high degree of accuracy.

Thermal Stress on Panels Caused by Cloud Transients: Cloud transients also impose a thermal stress cycle similar to that caused by daily operation. The dynamics of flow control, however, can affect the magnitude of the thermal stress cycle, since the stress depends on both the degree of cooling as well as the degree of heating the panel. Figure 16 presents the solar flux, salt flow, and a calculation of the thermal stress for a simulated east-to-west cloud transient. The values are presented as a percent of design values and are for a tube at the back (center) of the cavity, where the highest flux occurs. As solar flux returns, due to passage of the cloud, flow lags for a short time to allow the receiver to heat up. This results in a mismatch between solar heating and salt cooling that in turn results in a high thermal stress cycle. Work on the receiver's control algorithm is recommended to reduce this problem by forcing the salt's flow rate to "match" flux within certain limits, overriding normal temperature control during rapid transients. This will delay the return to a normal operating temperature, but will reduce the fatigue damage to the receiver's panel.

Thermal Expansion of the Panel: Measurements of the panel's growth during testing confirmed that the provisions for thermal expansion were adequate for both the Babcock & Wilcox and Foster Wheeler panel designs. The panel growth was between 1 and 2 cm (0.39 and 0.78 in.), depending upon the operating temperature, each time the receiver was started, and the panel returned its to normal position when the receiver was shut down. No evidence of binding of the lateral supports was detected.

Fabrication Methods: Two problems with the fabrication of the receiver became apparent during the test program. They were related to the welding of the tube-clips' support attachments and to details of the header's fabrication.

The tubes were attached to lateral supports by clips welded to the back of the tubes. Several of the welds developed pinhole salt leaks during the testing. Salt from the leaks migrated to the front of the tubes, causing discoloration of the black paint and some loss of absorptivity. Thirteen such blemishes occurred during the test program, affecting approximately 2% of the absorber surface. In future receivers, adherence to strict, well-controlled procedures and quality assurance in welding anything to the thin-walled tubes will be required to eliminate this problem.

FIGURE 15
HEAT FLUX LIMITS ON THE RECEIVER

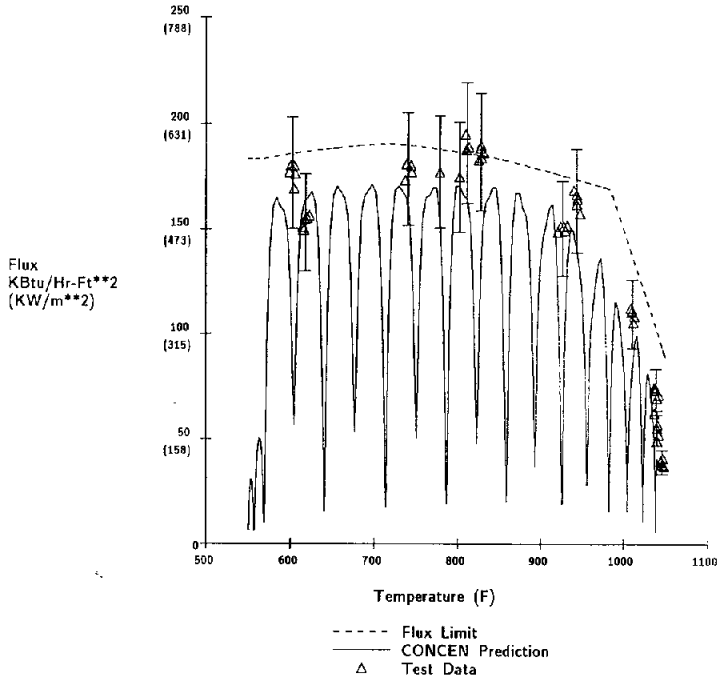

FIGURE 16
THERMAL STRESS CAUSED BY CLOUD TRANSIENTS

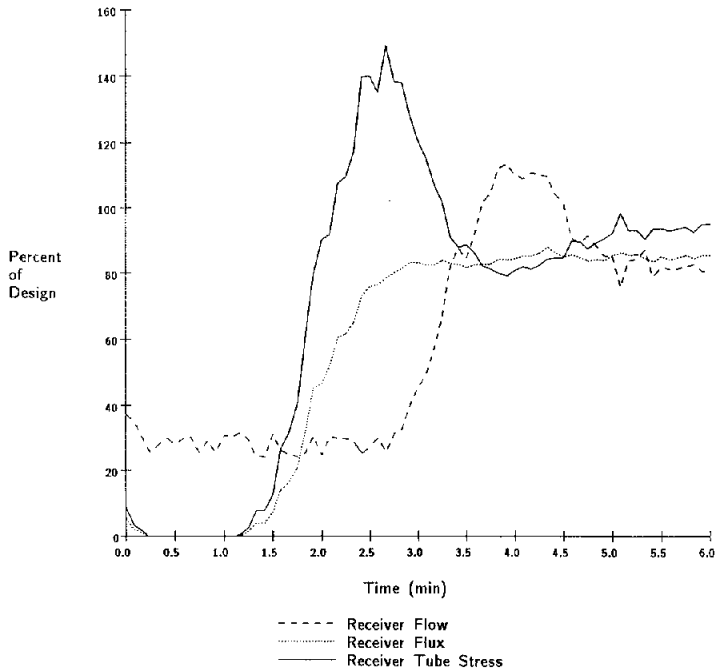

The tubes of each receiver's flow pass are welded into a common header at each end. This weld connection and the header itself must be designed for the thermal fatigue caused by rapid temperature transients caused by the salt. During testing, it was found that the temperature-rise rate limits imposed by the specific header designs employed in the test receiver were being exceeded during start-up and during operation with clouds. Test operations were altered to minimize this problem by applying power gradually during mid-day start-ups, but this increased start-up time and reduced energy collected by the receiver. In a future receiver, improvements in the header configuration should be made to allow the receiver to operate with sudden application of full solar power without causing thermal fatigue of the headers.

Evaluation of the Heat Trace: The heat-trace system worked adequately. The active heat-trace controls performed well, and the temperature of most components could be maintained in all weather conditions. The balance of the heat-trace power with thermal losses within a control zone was important; however, long runs of piping with different external conditions at each end developed large temperature differences and had to be overheated at one end to maintain the required temperature the other. Sensitive elements, such as pressure transmitter diaphragms, required individual controllers to prevent overheating. In general, good quality mineral-insulated (MI) cable heat-trace was found to be reliable, but occasional failures are unavoidable. The main drawback of MI cable is that, once failed, replacement is difficult, since it usually requires removal of insulation from long pipe runs. Heat-trace systems that are more easily replaced would probably be more expensive to install, but may be more economical in the long run when replacement costs are considered.

Instrumentation: The receiver's instrumentation (shown in Figure 12) allowed control and data acquisition for the test. The thermocouples, air-cooled flux gauges, displacement gauges, level sensor for the hot surge tank, and absolute pressure gauges performed well. Problems were experienced with the water-cooled flux gauges and the differential pressure transmitters used for flow measurement and level measurement in the cold surge tank. The water-cooled flux gauges tended to plug while in service because a very small flow passage was used and a small amount of solid deposit would plug the gauge. This is apparently a flaw in the design of the gauges, since there is no reason for such a small flow path for this application. The manufacturer has been consulted, and more freely flowing gauges are available. The differential pressure transmitters used for flow and level measurement employed oil-filled isolation diaphragms to transmit salt pressure to the gauge. The gauges experienced large calibration shifts with time, making them unreliable. The oil employed was Syltherm silicon oil. In order to prevent salt from freezing on the diaphragm, the diaphragms had to be heated to nearly the maximum rated oil temperature. It is recommended that alternate isolation fluids such as NaK be employed in future applications, or that alternative flow and level sensor methods be developed.

Overall, the design methods employed in this receiver were found to be valid. A few problems with the design were identified, but there appear to be no major design issues that would prevent scale-up of this receiver design.

5.2 Measurement of Thermal Performance

The receiver's efficiency, defined as the power absorbed in the molten salt divided by the power incident on the receiver's aperture, is the basic measure of the receiver's ability to collect solar energy. Because there is no good method to measure incident power, the receiver's efficiency is difficult to evaluate accurately. Two methods exist to calculate/estimate its efficiency. The first is the 'calculated input' method, which employs an analytical calculation of the collector field's input [13]. The second is the method of 'complementary collector partitions,' which infers thermal loss from the receiver's operation at different incident power levels [13]. Both methods were used to evaluate performance for this receiver.

Calculated Input (Using HELIOS): Measurements of the steady-state absorbed power are available for many days at even-hour increments from solar noon. These measurements are results of the steady-state tests. These data were normalized to May 31 and are representative of operation for a 12-hour day near spring equinox. For each data point, the incident power was calculated using a table of values generated using the HELIOS program. The incident field power is calculated by the HELIOS code in several steps. The gross field power is equal to the mirror area of the field times the normal insolation. This sum is then reduced by cosine losses due to the angle that each mirror must assume to reflect the sun's rays to the receiver, and shading and blocking effects of the adjacent heliostats. Then the reflectivity of the mirrors is taken into account, along with propagation losses between the mirror and the receiver. Finally, the flux falling outside the aperture (spillage) is deducted, leaving the incident power. Figure 17 shows the incident power and absorbed power for the receiver as a function of time of day.

Complementary Field Partitions (Flux-On Loss Testing): The method of complementary field partitions assumes that the receiver's losses are relatively constant. This is reasonable because they are, to a large extent, a function of the absorbing panel's temperature, and the panel's temperature is relatively constant. The panel's temperature stays constant because the salt's temperature is controlled at 565°C (1050°F), no matter what the input power is. If the receiver is operated with the full collector field, then with two halves of the field individually, the difference between the absorbed power from the full field and the sum of the part-field powers is the receiver's thermal loss. Baker [13] presents formulas to make corrections for variations in solar input and for the small variation in losses that occurs with incident power. This type of test was conducted five times in the test program. The results of these tests showed thermal losses ranging from 57 to 302 kW at full receiver power, the range being attributed to scatter in the data.

FIGURE 17
DAILY PERFORMANCE OF THE COLLECTOR FIELD AND RECEIVER

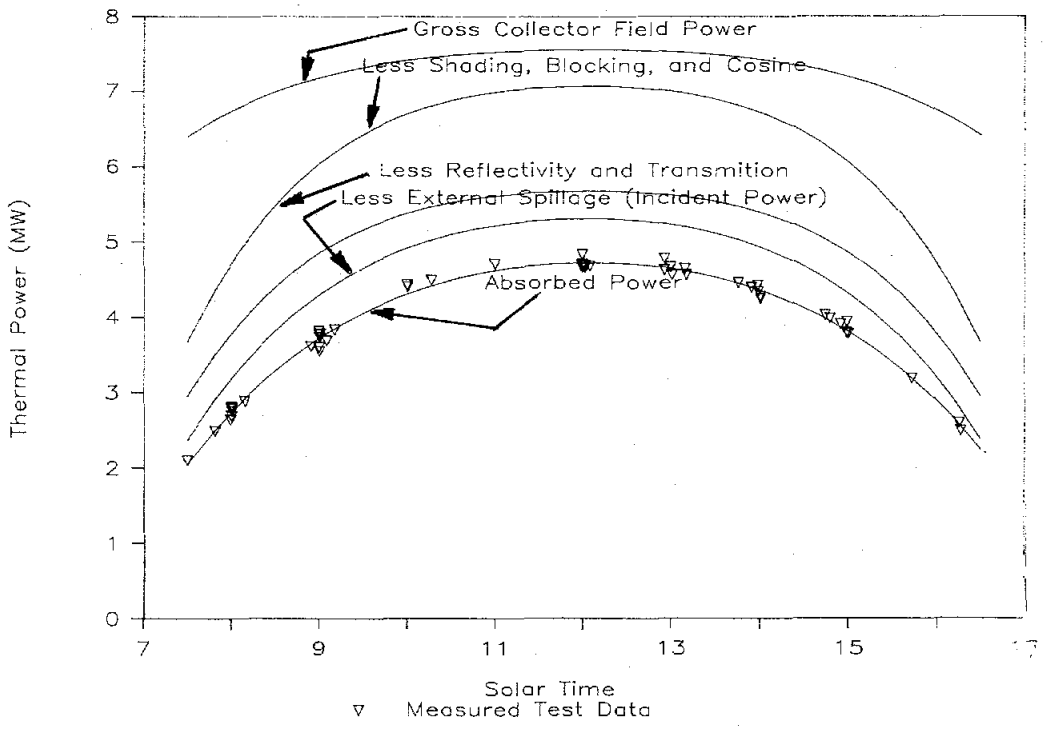

The receiver's efficiency can be calculated based on the losses determined by both methods. The calculated input method yields an efficiency of 91 ± 9% at solar noon, and the method of complementary partitions (flux-on test) gives an efficiency of 95 ± 8%. The uncertainty in the calculated input method is about equally divided between the uncertainty in the calculation of input power (largely spillage loss) and measurement of flow, all of which leads to uncertainty in the calculation of absorbed power. The uncertainty about efficiency in the flux-on test was largely a result of uncertainty about the flow rate. The basic flow rate uncertainty, however, is compounded with this method since the loss involves the combination of three calculations of absorbed power. The receiver's calculated efficiency based on both methods is presented in Figure 18 as a function of absorbed power, with an estimate of the experimental uncertainty. The uncertainty ranges for the two methods overlap, and it is expected that the true efficiency lies in this overlap. The measurements are consistent with the 90% efficiency originally expected for this design. Attempts to correlate the measured thermal efficiency with wind showed that the scatter in the data overwhelmed any discernible trend.

Integration of the thermal power produced during the 9 hours shown in Figure 17 yields an absorbed energy of 35.2 MWh. The receiver's average thermal efficiency for this period was 89%, based on the calculated input method.

FIGURE 18
THERMAL EFFICIENCY OF THE RECEIVER

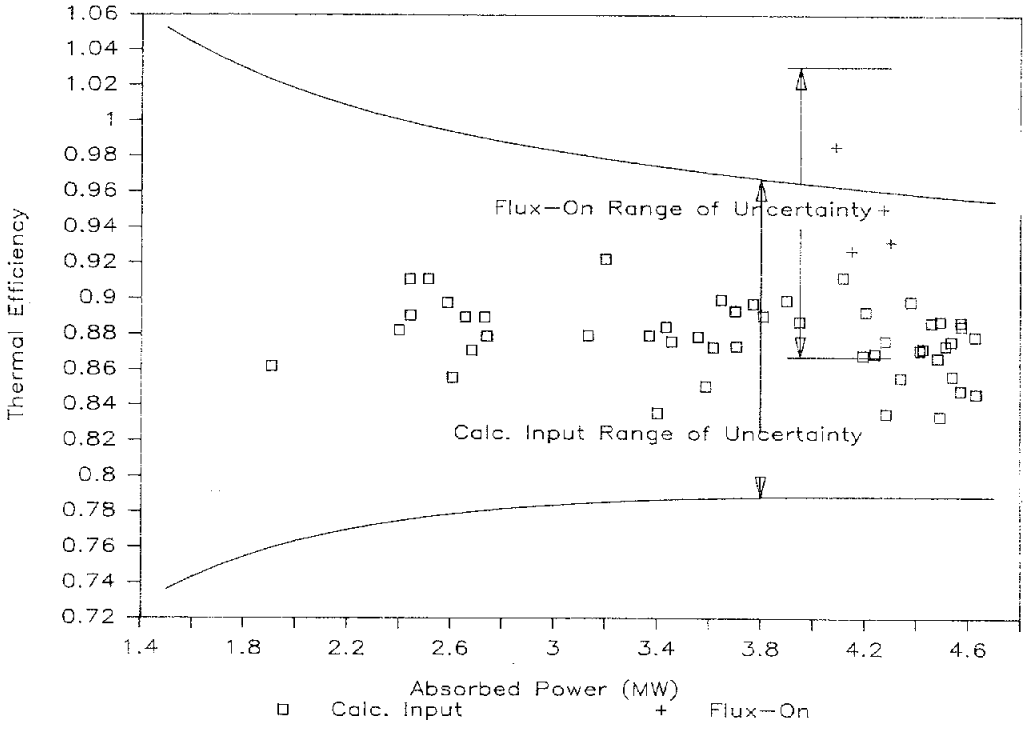

5.3 Definition of Capabilities

Possibly as important as efficiency relative to collecting energy is the capability of the receiver to start-up and collect energy during a variety of conditions. Rapid start-up allows maximum energy collection both at daybreak, or when cloudy conditions clear. The ability to start-up and operate in clouds allows collection of what may be a significant amount of energy on an annual basis. Start-up and controls performance are discussed in the following.

Start-Up Capabilities: To start the salt flow in the receiver, the tubes of the absorption panel must be hot to prevent the salt from freezing. The tubes were heated in two ways during the tests:

- By warming the panel with the collector field.
- By keeping the panel warm by heating the cavity with the door closed.

Using the heliostats to warm the panel at sunrise required 15 minutes to heat the panel, then another 21 minutes to establish the salt flow and bring the full collector field on-target. Once this was done, collection of useful energy began. The receiver had a controllable flow limit of 25% of full flow. As a result, the full outlet-temperature of 565°C (1050°F) was not reached until 90 minutes past sunrise, when the collector's power was high enough to achieve 25% of absorbed power. Lower temperature (less than 400°C (750°F)) salt generated during this time was diverted to the cold tank where it preheated the salt inventory slightly; 400-565°C (750-1050°F) salt went to the hot tank. In this way, the energy was retained as useful energy in the system. During these 90 minutes, 686 kWh of thermal energy was collected.

Heating the panel overnight allowed flow to be established and the collector field to be focused on the receiver at sunrise. This allowed 873 kWh of thermal energy to be collected in the first 90 minutes of operation, or 187 kWh more than with a solar start-up. Figures 19 and 20 present the receiver's power, and outlet-temperature, as a function of time past sunrise, based on test results.

Two methods were tested for overnight heating of the panels; electric cavity heaters and continuous salt circulation. Electric heaters consumed only 12 kW of electricity over a 12-hour night to keep the panels warm. The method greatly simplified start-up. Overall, however, this method costs more energy than it allows to be made up, given the conversion efficiency from thermal to electric energy. The heaters also proved useful for initial check-out of the receiver, as they allowed salt flow without the complication of solar operation.

The other method of heating the cavity is with continuous salt circulation. Once the receiver was started (using one of the other methods), salt flow was maintained after shutdown by circulating salt from the thermal storage system on the ground. This method not only kept the cavity warm, but also kept the receiver's piping hot, eliminating the need to operate the electric heat trace. Test results show that the heat-trace load can be reduced from 35 kW to approximately 5 kW with salt circulation. Piping in the tower is also kept hot by circulation, allowing another 30 kW to be saved. This test was conducted using the main salt pumps, which created a large pumping parasitic (approximately 130 kW). The pumps are required to operate with large throttling losses, far from their design point. It is estimated that pumps designed specifically for this purpose would consume only 12 kW.

Continuous circulation would also make it possible to start the process rapidly after cloudy conditions cleared and to operate on partially cloudy days when solar start-ups would be difficult. No testing was performed, however, to quantify this effect.

Performance of Receiver Controls: The main objective of the receiver's control system is to maintain the outlet-temperature of the receiver, maximize absorbed power, avoid overheating the salt and minimize the thermal fatigue of the receiver. In addition, the control system incorporates a number of 'trips', which cause the receiver to shut down when an unsafe condition is detected.

The receiver's control-algorithm employs signals from the flux gauges, thermocouples on the back of the absorber panel, and thermocouples in the outlet-salt flow. The receiver's flow control-algorithm uses the heat flux measurements and back tube temperatures as "feed forward signals" to anticipate outlet temperature and set the salt's flow rate accordingly. Outlet-temperature is used as a "feedback" signal to make adjustments in flow to achieve accurate outlet temperature control. During cloud transients, when incident flux falls below a minimum value, it becomes

FIGURE 19
ABSORBED POWER DURING MORNING START UP

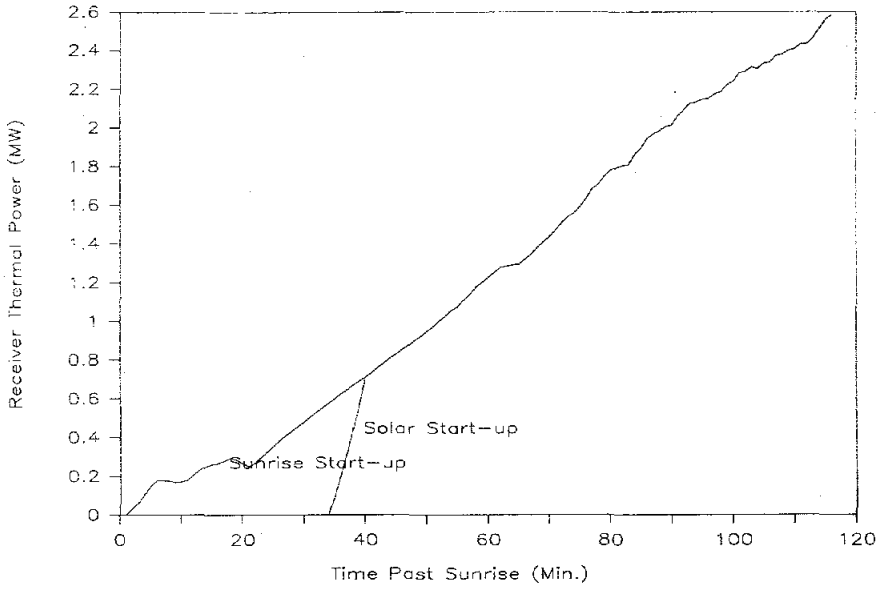

FIGURE 20
OUTLET TEMPERATURE DURING MORNING START UP

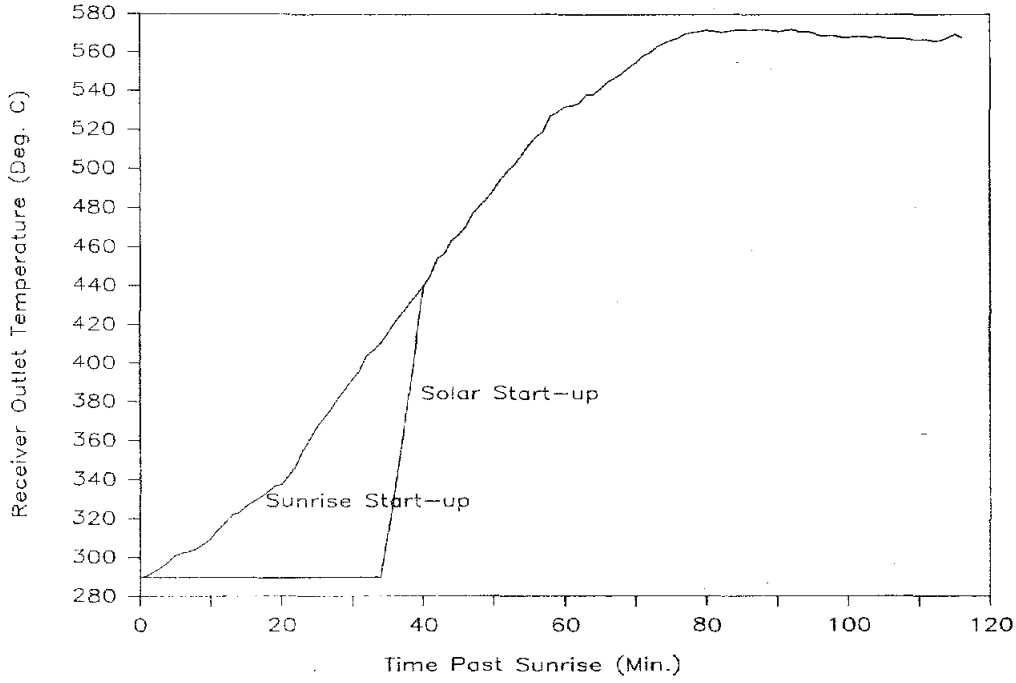

impossible to control outlet-temperature at the desired value, or "set-point." When this happens, the receiver's outlet temperature decays. The control-algorithm senses this and automatically lowers the outlet temperature set point. When the sun returns, the set-point rises gradually to the original setting to prevent the outlet-salt temperature from exceeding the salt's high temperature limit (593°C (1100°F)).

During cloudy conditions, the control algorithm performed well in utilizing the available solar power. An example of solar insolation during cloudy conditions is presented in Figure 21.

Although insolation varied significantly, approximately half-power conditions, on the average, existed throughout the morning on this day. The control system was able to maintain a somewhat degraded, but altogether acceptable outlet temperature while operating through the worst of these conditions, as shown in Figure 22. More important, continuous energy collection was maintained during this period, as shown in Figure 23, making maximum use of the solar energy falling on the collector field between clouds.

Overall, very good outlet-temperature control and energy collection were achieved with this receiver's control-algorithm. Outlet-temperature overshoot was limited to less than 17°C (30°F) in all types of natural clouds as well as for simulated worst case clouds. However, as noted in the previous section, cloud transients result in significant thermal stress cycles for the absorber panel, but improvements are currently being developed to minimize this problem.

FIGURE 21
DIRECT NORMAL SOLAR INSOLATION

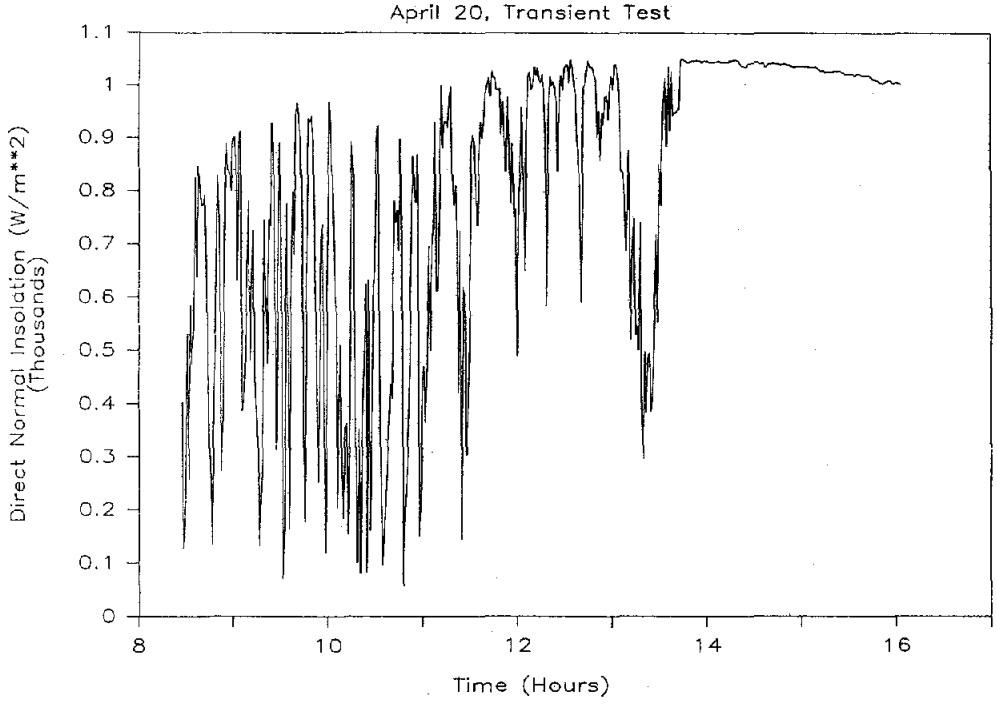

FIGURE 22
RECEIVER INLET AND OUTLET TEMPERATURES

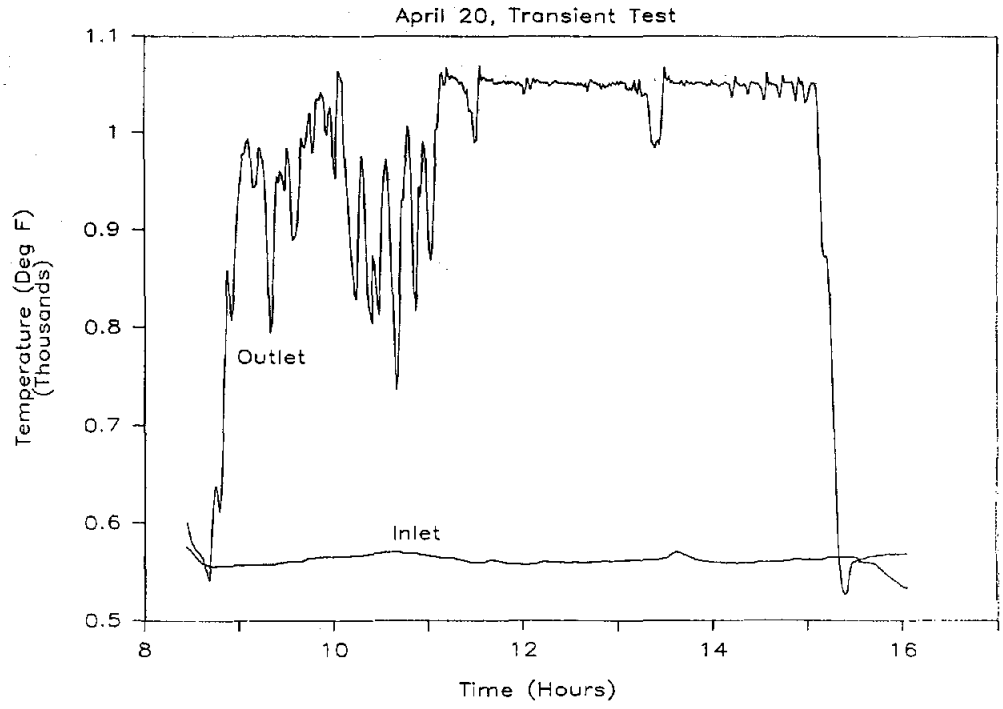

FIGURE 23
TOTAL ENERGY COLLECTION

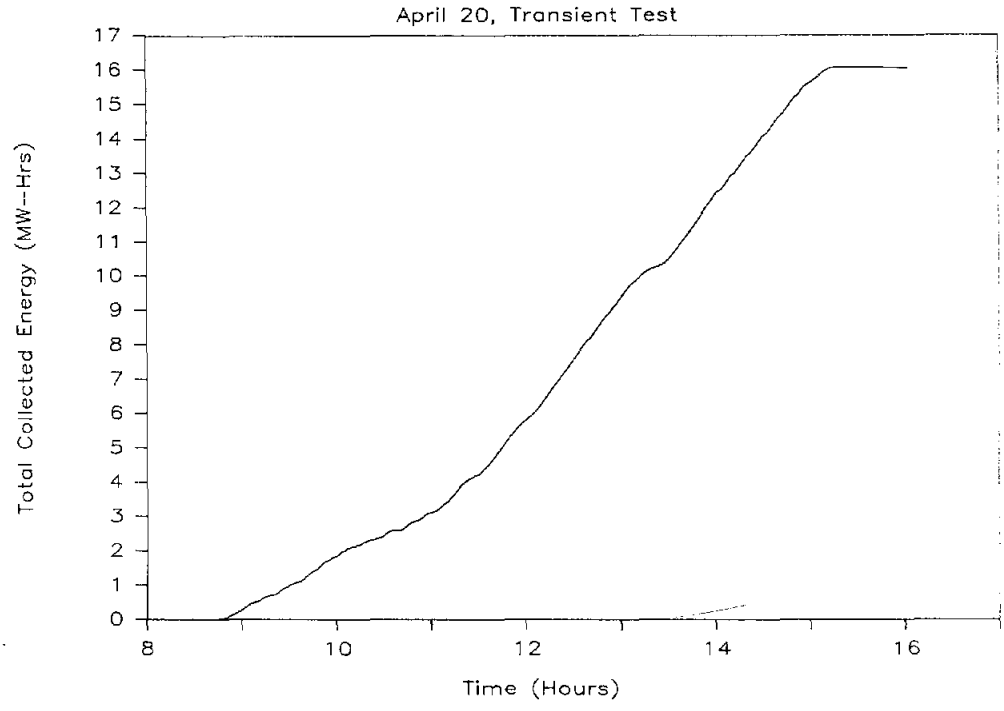

6.0 SUMMARY AND CONCLUSIONS

Overall, the test objectives were met, and the receiver performance was verified. In a few areas, however, problems were discovered and improvements are necessary. In most of these areas, the improvements appear to be straightforward, and no major obstacles were discovered to stand in the way of scaling up this basic receiver design.

Design Confirmation: The heat absorption panels performed well at steady-state operating conditions. Analysis of the test conditions indicate the temperatures and fatigue stress conditions show that the required receiver life is possible. Measurements during receiver transients revealed stresses that were much higher than anticipated during rapid cloud transients, and this could have a major impact on the fatigue life of the panels. This is a major area for continued study. The panel's support system performed well for both the Babcock & Wilcox and Foster Wheeler panels. The receiver's paint also performed well (final absorptance was 97%) and showed no indication of general degradation during the short test time. Two problems with fabrication of the panels were discovered that require improvements in commercial designs. First, tube-clip welding must be improved because thirteen pinhole leaks developed during the testing at tube-clip welds. Although they caused no significant operational problems, the minute quantity of salt that escaped did blemish the painted surface of the receiver. This was largely unsightly, but it could eventually affect the absorptivity of the receiver. Improved welding and inspection practices should solve this problem in future receivers. The panel headers were also found to have design and fabrication deficiencies that made them sensitive to the salt temperature rise rates experienced in partially cloudy conditions. Both the Babcock & Wilcox and Foster Wheeler headers had similar limitations, but for different reasons. The panel headers must be designed to accept rapid temperature transients in order to make maximum use of available solar energy. A design incorporating the best features of both headers tested would have ample limits to withstand the rapid temperature transients.

Major improvements in instrumentation and heat trace were demonstrated over previous molten salt receiver tests. Instrumentation for this receiver included solar heat-flux gauges. Passive air-cooled gauges performed well and contributed to a major improvement in receiver control. Water-cooled gauges had inadequate cooling and would need to be improved for future application. Flow measurement and level measurement in the pressurized surge tank were barely adequate for the test program. The sensitive differential pressure transmitters, upon which the test system depended, should be developed or alternate sensors need to be developed. The heat-trace system performed adequately as a result of the active control system employed. The salt containment and piping systems were heated and kept hot over a wide variety of conditions. However, heat trace continues to be the most maintenance-intensive aspect of the receiver subsystem. This could be a major problem in a commercial plant, and improvements to reduce maintenance of heat trace are needed.[10] Other support systems, such as the receiver door, piping, and bellows seal valves performed as expected, with no major problems.

Thermal Performance: Thermal performance testing of the receiver confirmed a high efficiency (approximately 90%) and therefore good capability to collect energy during clear conditions. Detailed modeling of the receiver was performed, and test results showed good agreement with the models.

Capabilities of the Receiver: The receiver also demonstrated the ability to make maximum use of solar energy available in non-steady-state conditions. This is made possible by the molten-salt storage system, which separates the receiver from the power-generation portion of the plant. Adequate controls, however, are required to make use of this energy. The controls strategy developed for this receiver demonstrated that maximum energy could be collected during all kinds of cloudy conditions, as well as for low-power, early-morning (and late-evening) operation. Improvements to achieve higher maximum to minimum flow (turn down) ratios should be pursued, in addition to improvements to minimize thermal stress of the receiver tubes. Thermal/hydraulic considerations allow a 5 to 3 turndown ratio for this receiver, but control tuning was performed for a less demanding 4 to 1 ratio. Further fine tuning would be required to achieve the full range. The original design of the control system placed a premium on achieving the rated salt outlet temperature. Testing revealed that trying to reach this temperature after a rapid cloud transient resulted in major fatigue cycles in the panel/headers. It is clear from these results that minimizing fatigue must also be a major goal of the control system. The flexibility offered by digital programmed control and solar flux measurements should make possible major improvements in this area.

Overall, the test was successful in demonstrating a mature salt-in-tube receiver design, ready for scale-up to larger systems. The test also served to reveal several critical areas that must be addressed in such a design to insure good performance and required receiver life, protecting the investment of developers and operators of future solar power systems.

This Page Intentionally Left Blank

REFERENCES

1. Weber, E.R., "Saguaro Power Plant Solar Repowering Project," DOE/SF10739-2, Arizona Public Service Company, Phoenix, Arizona, July 1980.

2. Ross, K., Roland, J., and Douma, J., "Solar 100-Conceptual Study," Southern California Edison Company, August 3, 1982.

3. Holl, R.J., Barron, D.R., and Saloff, S.A., McDonnell Douglas Astronautics Company, "Molten Salt Electric Experiment," Research Project RP2302-2, Electric Power Research Institute, Palo Alto, California, March 1987.

4. Martin Marietta Corporation, "Molten Salt Electric Experiment (MSEE), Phase I," SAND85-8175, Sandia National Laboratories, Albuquerque, New Mexico and Livermore, California, August 1985.

5. Weber, E.R., "Preliminary Design of a Solar Central Receiver for a Site Specific Repowering Application (Saguaro Power Plant)," DE-FC03-82SF11675-1, Arizona Public Service Company, Phoenix, Arizona, September 1983.

6. Maxwell, C., and Holmes, J., "Central Receiver Test Facility Experiment Manual," SAND86-1492, Sandia National Laboratories, Albuquerque, New Mexico and Livermore, California, January 1987.

7. Delameter, W.R., and Bergan, N.E., "Review of the Molten Salt Electric Experiment: A Solar Central Receiver Project," SAND86-8249, Sandia National Laboratories, Albuquerque, New Mexico and Livermore, California, December 1986.

8. The Babcock and Wilcox Company, "Molten Salt Electric Experiment Steam Generator Subsystem Final Report," SAND85-8181, Sandia National Laboratories, Albuquerque, New Mexico and Livermore, California, April 1986.

9. Nelson, C. and Mahoney, R.A., "The Effect of Vitrification Temperature Upon the Solar Average Absorptance Properties of Pyromark Series 2500 Black Paint," SAND86-0675, Sandia National Laboratories, Albuquerque, New Mexico and Livermore, California, June 1986.

10. Holmes, J. T., "Electric Heating for High-Temperature Heat Transport Fluids," SAND85-0379, Sandia National Laboratories, Albuquerque, December 1985.

11. "Criteria for Design of Elevated Temperature Class 1 Components in Section III, Division 1 of the ASME Boiler and Pressure Vessel Code," May 1986.

12. Kistler, B.L., "Fatigue Analysis of a Solar Central Receiver Design Using Measured Weather Data," SAND86-8017, Sandia National Laboratories, Livermore, California, to be published.

13. Jones, W.B., Bourcier, R.J., "Thermal Fatigue of Solar Receiver Candidate Alloys," Proceedings of the DOE Solar Central Receiver Technical Annual Meeting, SAND85-8241, Sandia National Laboratories, Albuquerque, NM, December 1985.

14. Baker, A.F., "International Energy Agency (IEA) Small Solar Power Systems (SSPS) Sodium Cavity and External Receiver Performance Comparison," SAND87-8021, Sandia National Laboratories, Albuquerque, New Mexico and Livermore, California, October 1987.

UNLIMITED RELEASE
INITIAL DISTRIBUTION

U.S. Department of Energy (6)
Forrestal Building
Code CE-314
1000 Independence Avenue, SW
Washington, DC 20585
Attn: H. Coleman
S. Gronich
F. Morse
M. Scheve
R. Shivers
T. Wilkins

U.S. Department of Energy
Forrestal Building
Code CE-33
1000 Independence Avenue, SW
Washington, DC 20585
Attn: C. Carwile

U. S. Department of Energy
CE-1, Forrestal
1000 Independence Avenue, Sw
Washington, DC 20585
Attn: D. Fitzpatrick

U.S. Department of Energy
Albuquerque Operations Office
P.O. Box 5400
Albuquerque, NM 87115
Attn: D. Graves

U.S. Department of Energy
San Francisco Operations Office
1333 Broadway
Oakland, CA 94612
Attn: R. Hughey

Advanced Controls & Automation
7200 Montgomery NE, Suite 169
Albuquerque, NM 87109
Attn: G. Riley

Advanced Thermal Systems
7600 East Arapahoe
Suite 319
Englewood, CO 80112
Attn: D. Gorman

Analysis Review & Critique
6503 81st Street
Cabin John, MD 20818
Attn: C. LaPorta

Arizona Public Service Company
P.O. Box 21666
Phoenix, AZ 85036
Attn: J. McGuirk

Arizona Solar Energy Office
Dept. of Commerce
1700 W. Washington, 5th Floor
Phoenix, AZ 85007
Attn: Dr. Frank Mancini

Asinel
Francisco Gervas, 3
Madrid 28020
Spain
Attn: Jesús M. Mateos

Atlantis Energy Ltd.
Thunstrasse 43a
3005 Bern, Switzerland
Attn: Mario Posnansky

Babcock and Wilcox
91 Stirling Avenue
Barberton, OH 44203
Attn: D. Young

Battelle Pacific Northwest (2)
Laboratory
P.O. Box 999
Richland, WA 99352
Attn: T. A. Williams
K. Drost

Bechtel National, Inc. (4)
50 Beale Street
50/15 D8
P. O. Box 3965
San Francisco, CA 94106
Attn: P. DeLaquil
B. Kelly
J. Egan
R. Leslie

Black & Veatch Consulting
Engineers (4)
P.O. Box 8405
Kansas City, MO 64114
Attn: J. C. Grosskreutz
J. E. Harder
L. Stoddard
J. Arroyo

Tom Brumleve
1512 Northgate Road
Walnut Creek, CA 94598

California Energy Commission
1516 Ninth Street, M-S 43
Sacramento, CA 95814
Attn: A. Jenkins

California Public Utilities Com.
Resource Branch, Room 5198
455 Golden Gate Avenue
San Francisco, CA 94102
Attn: T. Thompson

Centro Investigations Energetica (3)
Medroansental Technologie (CIEMAT)
Avda. Complutense, 22
28040 Madrid
SPAIN
Attn: L. Crespo
F. Sanchez
M. Romero

Conphoebus
Sede Leg.
Via G. Leopardi, 60
95127 Catania
ITALY
Attn: Gino Beer

DFVLR
IEA/SSPS Project
Apartado 649, E-04080
Almeria, SPAIN
Attn: M. Geyer

DFVLR EN-TT (2)
Institute for Technical
Thermodynamics
Pfaffenwaldring 38-40
7000 Stuttgart 80
Federal Republic of Germany
Attn: Dr. C. Winter
Dr. M. Fisher

DFVLR, HA-ET (3)
Linder Hoehe
5000 Cologne 90
Federal Republic of Germany
Attn: M. Becker
M. Boehmer
U. Nikolai

EIR
CH-5303 Wurenlingen
Switzerland
Attn: W. Durish

El Paso Electric Company
P.O. Box 982
El Paso, TX 79946
Attn: J. E. Brown

Electric Power Research
Institute (2)
P.O. Box 10412
Palo Alto, CA 94303
Attn: J. Bigger
E. DeMeo

Engineering Perspectives
20 19th Avenue
San Francisco, CA 94121
Attn: John Doyle

Foster Wheeler Solar Development
Corporation (2)
12 Peach Tree Hill Road
Livingston, NJ 07039
Attn: S. F. Wu
R. Zoschak

Georgia Institute of Technology
GTRI/EMSL Solar Site
Atlanta, GA 30332
Attn: T. Brown

Georgia Power
7 Solar Circle
Shenandoah, GA 30265
Attn: Ed. Ney

Leo Gutierrez
434 School Street
Livermore, CA 94550

HGH Enterprises, Inc.
23011 Moulton Parkway
Suite C-13
Laguna Hills, CA 92653
Attn: Dick Holl

Interatom GmbH
P. O. Box
D-5060 Bergisch-Gladbach
Fededral Republic of Germany
Attn: M. Kiera

Lawrence Berkeley Laboratory
MS 90-2024
One Cyclotron Road
Berkeley, CA 94720
Attn: Arlon Hunt

Los Angeles Department of Water
and Power
Alternate Energy Systems
Room 661A
111 North Hope Street
Los Angeles, CA 90012
Attn: Bill Engels

Luz International (2)
924 Westwood Blvd.
Los Angeles, CA 90024
Attn: D. Kearney
M. Lotker

McDonnell Douglas
Astronautic Corporation
M.S. 49-2
5301 Bolsa Avenue
Huntington Beach, CA 92613

Nevada Power Co.
P. O. Box 230
Las Vegas, NV 89151
Attn: Mark Shank

Platforma Solar de Almeria (2)
Aptdo. 7
Tabernas (Almeria)
E-04200 Spain
Attn: A. Sevilla
M. Silva

Public Service Company of New Mexico
M/S 0160
Alvarado Square
Albuquerque, NM 87158
Attn: T. Ussery
A. Martinez

Pacific Gas and Electric Company (3)
3400 Crow Canyon Road
San Ramon, CA 94526
Attn: G. Braun
T. Hillesland
B. Norris

Polydyne, Inc.
1900 S. Norfolk Street, Suite 209
San Mateo, CA 94403
Attn: P. Bos

Public Service Company of Colorado
System Planning
5909 E 38th Avenue
Denver, CO 80207
Attn: D. Smith

Ramada Energy Systems Ltd.
1421 S. McClintock Drive
Tempe, AZ 85281
Attn: R. Bingman

San Diego Gas and Electric Company
P.O. Box 1831
San Diego, CA 92112
Attn: R. Figueroa

SCE
P. O. Box 800
Rosemead, CA 91770
Attn: W. vonKleinSmid

Sci-Tech International
Advanced Alternative Energy
Solutions
5673 W. Las Positas Boulevard
Suite 205
P.O. Box 5246
Pleasanton, CA 84566
Attn: Ugur Ortabasi

Science Applications International
Corporation
2109 Airpark Road, SE
Albuquerque, NM 87106
Attn: D. Smith

Science Applications International
Corporation
10401 Roselle Street
San Diego, CA 92121
Attn: B. Butler

Solar Energy Research Institute (4)
1617 Cole Boulevard
Golden, CO 80401
Attn: M. Bohn
B. Gupta
J. Anderson
M. Carasso

Solar Kinetics, Inc. (2)
P.O. Box 540636
Dallas, TX 75354-0636
Attn: J. A. Hutchison
D. White

Solar Power Engineering Company
P.O. Box 91
Morrison, CO 80465
Attn: H. C. Wroton

Southern California Edison
P.O. Box 325
Daggett, CA 92327
Attn: C. Lopez

Stearns Catalytic Corporation
P.O. Box 5888
Denver, CO 80217
Attn: T. E. Olson

Stone and Webster Engineering
Corporation
P.O. Box 1214
Boston, MA 02107
Attn: R. W. Kuhr

Sulzer Bros, Ltd.
New Technologies
CH-8401 Winterthur
Switzerland
Attn: Hans Fricker, Manager

Tom Tracey
6922 South Adams Way
Littleton, CO 80122

United Solar Tech, Inc.
3434 Martin Way
Olympia, WA 98506
Attn: R. J. Kelley

University of Arizona
Engineering Experimental Station
Harvil Bldg., Room 151-D
Tucson, AZ 85721
Attn: Don Osborne

University of Houston (3)
Solar Energy Laboratory
4800 Calhoun
Houston, TX 77704
Attn: A. F. Hildebrandt
L. Vant-Hull
C. Pitman

University of Utah
Mechanical and Industrial
Engineering
Salt Lake City, UT 84112
Attn: B. Boehm

Eric Weber
302 Caribbean Lane
Phoenix, AZ 85022

400	J. A. Leonard
3141	S. A. Landenberger (5)
3151	W. I. Klein (3)
3154	C. L. Ward (8)
	For DOE/OSTI
6200	V. L. Dugan
6220	D. G. Schueler
6221	E. C. Boes
6222	J. V. Otts
6222	K. R. Boldt
6222	W. A. Couch
6223	G. J. Jones
6224	D. E. Arvizu
6226	J. T. Holmes
6226	D. J. Alpert
6226	J. M. Chavez (20)
6226	J. W. Grossman
6226	D. K. Johnson
6226	G. J. Kolb
6226	D. F. Menicucci
6226	C. E. Tyner
6227	P. C. Klimas
8024	P. W. Dean
8132	W. R. Delameter
8133	A. C. Skinrood
8151	A. F. Baker
8363	N. E. Bergan
8524	J. A. Wackerly